

## The Nature of SN 1961V

You-Hua Chu<sup>1</sup>, Robert A. Gruendl<sup>1</sup>, Christopher J. Stockdale<sup>2</sup>, Michael P. Rupen<sup>3</sup>, John J. Cowan<sup>4</sup>, Scott W. Teare<sup>5</sup>

### ABSTRACT

The nature of SN 1961V has been uncertain. Its peculiar optical light curve and slow expansion velocity are similar to those of super-outbursts of luminous blue variables (LBVs), but its nonthermal radio spectral index and declining radio luminosity are consistent with decades-old supernovae (SNe). We have obtained *Hubble Space Telescope* STIS images and spectra of the stars in the vicinity of SN 1961V, and find Object 7 identified by Filippenko et al. to be the closest to the optical and radio positions of SN 1961V. Object 7 is the only point source detected in our STIS spectra and only its H $\alpha$  emission is detected; it cannot be the SN or its remnant because of the absence of forbidden lines. While the H $\alpha$  line profile of Object 7 is remarkably similar to that of  $\eta$  Car, the blue color (similar to an A2 Ib supergiant) and lack of appreciable variability are unlike known post-outburst LBVs. We have also obtained Very Long Baseline Array (VLBA) observations of SN 1961V at 18 cm. The non-detection of SN 1961V places a lower limit on the size of the radio-emitting region, 7.6 mas or 0.34 pc, which implies an average expansion velocity in excess of 4,400 km s<sup>-1</sup>, much higher than the optical expansion velocity measured in 1961. We conclude the following: (1) A SN occurred in the vicinity of SN 1961V a few decades ago. (2) If the SN 1961V light maximum originates from a giant eruption of a massive star, Object 7 is the most probable candidate for the survivor, but its blue color and

---

<sup>1</sup>Astronomy Department, University of Illinois, 1002 W. Green Street, Urbana, IL 61801; chu@astro.uiuc.edu, gruendl@astro.uiuc.edu

<sup>2</sup>Department of Physics, Marquette University, PO Box 1881, Milwaukee, WI 53201-1881; christopher.stockdale@mu.edu

<sup>3</sup>National Radio Astronomical Observatories, PO Box 0, 1003 Lopezville Road, Socorro, NM 87801-0387; mrupen@nrao.edu

<sup>4</sup>Department of Physics and Astronomy, University of Oklahoma, 440 West Brooks, Room 131, Norman, OK 73019; cowan@mail.nhn.ou.edu

<sup>5</sup>Department of Electrical Engineering, New Mexico Tech, 801 Leroy Place, Socorro, NM 87801; teare@nmt.edu

lack of significant variability are different from a post-outburst  $\eta$  Car. (3) The radio SN and Object 7 could be physically associated with each other through a binary system. (4) Object 7 needs to be monitored to determine its nature and relationship to SN 1961V.

*Subject headings:* supernovae: general – supernovae: individual (SN 1961V) – supergiants – galaxies: individual (NGC 1058) – radio continuum

## 1. Introduction

SN 1961V in the outskirts of the Sc galaxy NGC 1058 (distance = 9.3 Mpc; Tully 1980; Silbermann et al. 1996) is the prototype of Zwicky’s Type V supernovae (SNe), which are now classified as Type II Peculiar SNe. SN 1961V was unusual in many respects (Branch & Greenstein 1971). First, SN 1961V is one of the very few SNe whose progenitors are known. The progenitor of SN 1961V was visible as an 18 mag star from 1937 to 1960 (Zwicky 1964). Second, the optical light curve of SN 1961V was more complex and much broader than any other SN ever observed. It peaked at  $\sim 12$  mag in late 1961, remained visible for several years, and faded to 21.7 mag in 1970 (Branch & Greenstein 1971; Bertola & Arp 1970). Third, the initial expansion velocity of SN 1961V, 2,000–3,000 km s<sup>-1</sup>, was much lower than the typical expansion velocity of 15,000–20,000 km s<sup>-1</sup> for most SNe (Zwicky 1964; Branch & Greenstein 1971).

These peculiar properties of SN 1961V have raised skepticism concerning its nature as a SN. Based on the extended optical light curve and the anomalously low expansion velocity, Goodrich et al. (1989) suggested that SN 1961V was a luminous blue variable (LBV) similar to  $\eta$  Car, and its “SN explosion” was actually a super-outburst. Filippenko et al. (1995) obtained *Hubble Space Telescope* (*HST*) WFC1 images of SN 1961V and identified a red star with  $R = 24.55$ , their Object 6, as a candidate for the LBV survivor. Using archival *HST* WFPC2 images, Van Dyk, Filippenko, & Li (2002) suggested a fainter and redder star as an alternative candidate for the LBV survivor and called it Object 11 as an extension of the Filippenko et al. (1995) object list. The LBV hypothesis cannot explain, however, the nonthermal radio spectral index of SN 1961V,  $-0.4 \pm 0.3$  (Cowan, Henry, & Branch 1988) or  $-0.79 \pm 0.23$  (Stockdale et al. 2001b). The radio emission from  $\eta$  Car and its ejecta is thermal and optically thick, as it shows a positive spectral index and a complete lack of polarization (Duncan et al. 1995; Duncan, White, & Lim 1997). Furthermore, SN 1961V is more than 1,000 times more luminous than  $\eta$  Car at 20-cm wavelength (Retallack 1983; Stockdale et al. 2001b) and its radio light curve is similar to those of radio SNe (Stockdale et al. 2001a).

Existent images of SN 1961V show a complex environment. Narrow-band, emission-line images reveal two H II regions within  $3''$  to the north of SN 1961V (Fesen 1985; Cowan et al. 1988), while broad-band continuum *HST* WFC1 images show massive stars in and around the H II regions and in the vicinity of SN 1961V (Filippenko et al. 1995). SN 1961V is clearly associated with a star-forming environment, where SNe are expected to occur. Indeed, radio observations (Cowan et al. 1988; Stockdale et al. 2001b) show a nonthermal source at the south edge of the eastern H II region, coincident to within  $1''$  of the optical position of SN 1961V, and a fainter nonthermal radio source in the western H II region, corresponding to an unrelated supernova remnant (SNR).

To determine the nature of SN 1961V, it is crucial to recover the optical counterpart of SN 1961V with a high degree of certainty, and to determine spectroscopically whether it is a surviving LBV or a SN turning into a SNR. Thus, we have obtained *HST* imaging and spectroscopic observations of SN 1961V. We have also obtained high-resolution radio observations to determine the size of the radio source at SN 1961V. This paper reports these observations of SN 1961V and our analysis of its nature.

## 2. Observations and Reduction

### 2.1. HST STIS Observations

SN 1961V was observed with the *Hubble Space Telescope* Imaging Spectrograph (STIS) on 2002 October 23. Medium-resolution optical spectra were obtained with the G430M and G750M gratings tilted to observe the spectral ranges centered at  $4961 \text{ \AA}$  and  $6581 \text{ \AA}$ , respectively. The wavelength coverage and spectral resolution of the resulting spectrograms are  $4800\text{--}5125 \text{ \AA}$  and  $\sim 0.8 \text{ \AA}$  for the G430M grating, and  $6250\text{--}6900 \text{ \AA}$  and  $\sim 1.3 \text{ \AA}$  for the G750M grating. The  $52'' \times 2''$  slit was used in order to obtain “slitless” spectra of multiple sources simultaneously. The long dimension of the slit was oriented along a position angle of  $139^\circ.6$  to optimize the projected separations among the candidates of SN 1961V’s optical counterpart, minimizing the confusion from overlapping spectra.

The target position was acquired by peaking up on a nearby star and then offsetting to the location of SN 1961V. Spectrograms were then obtained using CR-SPLIT=4 for a total exposure time of 4,377 and 3,902 s for the G750M and G430M gratings, respectively. In between the spectroscopic observations, a deep image of the field with the 50CCD aperture and no filter was obtained for comparison with the spectroscopic observations. This imaging observation also used a CR-SPLIT=4 and had a total integration time of 1,800 s.

The raw observations were reduced using the STSDAS v3.0 and CALSTIS v2.3 utilities

within IRAF. For this reduction the best reference files were obtained from the Multimission Archive at Space Telescope. The sources in the field are too faint for the observations to be dithered to aid in the rejection of hot/warm pixels in the STIS/CCD images/spectra; therefore, the standard reduction pipeline was used with some attempt made to construct a better dark frame than was available. The raw dark frames obtained as part of the STIS calibration programs 9605 and 9612, which occurred closest in time to our STIS observations, were uploaded and combined. We found that even restricting the darks used to those from the five days bracketing our observations did not improve our image quality. We also investigated making changes to the standard pipeline processing where the dark frame was scaled to account for the difference in exposure time and CCD housing temperature. We found that a slight improvement to the image quality could be made by reducing the pipeline’s default scaling of the darks by 10% for our imaging data and 2% for our spectroscopic data. The effect of these changes is to minimize the excursions of improperly subtracted hot pixels from the median value in the frame.

An astrometric solution in the ICRS 2000.0 frame for the STIS/CCD image of the region around SN 1961V was obtained by first finding an astrometric solution for a WFPC2 image taken with the F606W filter as part of program 5446. This astrometric solution for the WFPC2 image is based on the positions of 7 stars with low proper motions from the USNO B1.0 catalog and has an accuracy of better than  $0''.2$  based on the residuals of the least squares fit to the stellar positions. We then used 19 point sources that appear in both the WFPC2 and STIS images to obtain a bootstrapped astrometric solution for the STIS image. The accuracy of the astrometry for the STIS image is estimated to be  $\sim 0''.25$  based on the rms of the residuals from the least squares fit bootstrap solution added in quadrature to the uncertainty for the astrometric solution for the WFPC2 image.

## 2.2. VLBA Observations

We have made high-resolution radio observations of SN 1961V using the Very Long Baseline Array (VLBA)<sup>1</sup>. The observations were made at 18 cm on 1999 September 14. 3C286 and 3C48 were used for flux calibration and J0253+3835 was used for phase calibration (Perley, Butler, & Zijlstra 2004). SN 1961V is a weak source for the VLBA (Cowan et al. 1988), so the phased Very Large Array (VLA) in its A-configuration, the longest baseline mode, was included to improve the sensitivity. The 27 VLA antennae were phased and

---

<sup>1</sup>The National Radio Astronomy Observatory is a facility of the National Science Foundation operated under a cooperative agreement by Associated Universities, Inc.

sampled every 10 seconds, and this sampling rate was used for the Very Long Baseline Interferometry (VLBI) data set. The data set was averaged in frequency to a total of 8 intermediate frequencies (IF's). We iteratively self-calibrated the VLBA observations of J0253+3835 for a single IF to produce a common amplitude scale, and this model was applied to the other IF's to produce a VLBA phase solution. The VLBA and VLA observations of J0253+3835 were then combined and self-calibrated further to achieve the best possible VLBI phase solutions. For a consistency check of our phase solution, embedded scans of a secondary calibrator, J0230+4032, were obtained throughout the course of the observations of SN 1961V.

The VLBI phase solution was applied to the observations and the resulting visibilities were Fourier transformed to obtain an image of SN 1961V. The synthesized beam size for this VLBI image was  $11.5 \text{ mas} \times 7.56 \text{ mas}$ , and the rms noise in the map was  $0.030 \text{ mJy beam}^{-1}$ . No compact or diffuse sources were detected with  $\geq 3\sigma$  confidence within 100 mas of the radio position of SN 1961V, at which the simultaneous VLA observations detected  $0.147 \pm 0.026 \text{ mJy beam}^{-1}$  for a synthesized beam of  $1''.20 \times 1''.01$  (Stockdale et al. 2001b). To reconcile the VLA detection and VLBI non-detection, the radio emission must be distributed over an area greater than the VLBI synthesized beam, i.e.,  $> 7.56 \text{ mas}$ .

### 3. Discussion

#### 3.1. Stellar and Interstellar Environment of SN 1961V

The broad-band STIS image in Figure 1 represents the deepest high-resolution image of SN 1961V and its surroundings ever obtained. In addition to the eleven bright stellar objects identified by Filippenko et al. (1995) and Van Dyk et al. (2002), many fainter stars are also detected. These eleven bright objects, marked in Figure 1c, are mostly supergiants with  $V = 24$  to  $25.5$ . To illustrate the position of SN 1961V, radio contours extracted from the Stockdale et al. (2001b) 18 cm VLA map are plotted over the STIS image in Figure 1d. The eastern radio source corresponds to SN 1961V, and our new astrometric calibration (§2.1) now places Object 7 the closest to SN 1961V. Three nebular arcs are visible and form an apparent supershell structure about  $5''.3 \times 3''.0$  (or  $240 \text{ pc} \times 135 \text{ pc}$ ) in size. Encompassed within the supershell are SN 1961V and Objects 6, 7, 9, and 11, while projected along the supershell rim are Objects 5, 8, and 10.

To date, the best narrow-band images of SN 1961V are still those obtained by Fesen (1985) using the Kitt Peak 2.1 m telescope. His red continuum image had a limiting magnitude of  $\sim 21$  mag, so it did not detect any of the stars in the vicinity of SN 1961V shown in

our STIS image. Two H II regions are detected in the [O III] image, but they appear better resolved in the H $\alpha$ + [N II] image: the eastern H II region consists of a bright diffuse emission region and two faint emission knots to the south, while the western H II region is resolved into two emission patches with similar brightnesses.

Comparisons between our STIS image and Fesen’s narrow-band images show the following correspondences. The bright diffuse emission from the eastern H II region is centered on the bright Object 8 projected against the northeast rim of the supershell, and the two H $\alpha$ -emission knots in the southern extension are coincident with Object 7 inside the supershell and Object 5 along the south rim of the supershell, respectively. In the western H II region, the eastern emission patch is coincident with the bright Object 10, but the western emission patch has no detectable stellar counterparts in our STIS image. The image of Object 10 is elongated and somewhat resolved, indicating that it consists of multiple stars; its location inside an H II region further indicates that it contains a group of massive stars. The stars in Object 10 are probably at least a few Myr old, as they are coincident with a radio SNR identified by Stockdale et al. (2001b), the western radio source in Figure 1d.

In summary, the STIS image illustrates that SN 1961V is associated with a complex, extended star forming region. It is projected within the central cavity of a supershell, with bright H II regions distributed along the shell rim. The presence of both H II regions and SNRs indicates that a mixture of stellar populations at different ages exist within  $\sim 100$  pc of SN 1961V.

### 3.2. The Optical Counterpart of SN 1961V

The optical position of SN 1961V was determined by Klemola (1986) to an accuracy better than  $0''.1$ , and this position is coincident with a fading nonthermal radio source (Branch & Cowan 1985; Cowan et al. 1988; Stockdale et al. 2001b). As shown in Figure 1d, Object 7 is the closest to SN 1961V, the eastern radio source.

Our long-slit STIS spectroscopic observations have been designed to detect line emission, as the stellar sources are faint and the detection of their continuum requires unrealistically long exposures. Of all stellar sources in the slit, only one is detected in H $\alpha$  emission (see Fig. 2). Aligning the STIS direct image with the H $\alpha$  spectrogram, we find that the point source corresponds to Object 7. The wavelength scale in Figure 2 is calibrated for the slit center; as Object 7 is offset by  $0''.46$  from the slit center, a wavelength correction of  $-5.1 \text{ \AA}$

should be applied.<sup>2</sup> The corrected wavelength of the H $\alpha$  emission from Object 7 corresponds to a heliocentric velocity of  $V_{\text{hel}} = 520 \pm 10 \text{ km s}^{-1}$ , which is consistent with the systemic velocity of the H II regions near SN 1961V measured by Gruendl et al. (2002). The H $\alpha$  line profile of Object 7, shown in Figure 3, appears to have a narrow core and broad wings, which can be measured up to  $\pm 550 \text{ km s}^{-1}$  (limited by the noise level of the spectrum). The absence of forbidden lines such as [O I]  $\lambda 6300$  and [O III]  $\lambda 5007$  indicates that the H $\alpha$  emission is stellar as opposed to originating from a SN/SNR transition object like SN 1979C or SN 1980K (Fesen et al. 1999).

Our STIS spectrograms also detected a patch of diffuse emission in the H $\alpha$  and [O III]  $\lambda\lambda 4959, 5007$  lines. This emission originates from the northwest rim of the supershell and corresponds to the northern part of the western H II region identified by Fesen (1985). The velocity of this diffuse emission cannot be accurately determined, but is consistent with  $V_{\text{hel}} \sim 520 \text{ km s}^{-1}$ .

### 3.3. Radio Properties of SN 1961V

Recent VLA observations of SN 1961V (Stockdale et al. 2001b) show that it is a non-thermal radio source with a spectral index of  $\alpha = -0.79 \pm 0.23$  ( $S_\nu \propto \nu^\alpha$ ) and a time decay index of  $\beta = -0.69 \pm 0.23$  at  $\sim 20 \text{ cm}$  ( $S_\nu \propto t^\beta$ ). The spectral and temporal properties of SN 1961V are consistent with other decades-old radio SNe, for example, SNe 1970G, 1957D, and 1950B (Stockdale et al. 2001a; Stockdale 2001). These properties are not consistent with radio observations of LBVs, which have an overall flat radio spectrum when convolved to the VLA resolution limit of SN 1961V, for example, AG Car, He 3-519, HR Car, WRA 751, P Cyg, and  $\eta$  Car (Duncan & White 2002, 2003; Retallack 1983; Duncan et al. 1997).

A more apt radio comparison may be made with SN 1954J in NGC 2403 (3.2 Mpc; Freedman et al. 2001), which has been established to be an outburst of the LBV “Variable 12”, misidentified as a SN (Humphreys & Davidson 1994; Smith, Humphreys, & Gehrz 2001). The region near SN 1954J was observed with the VLA at 20 cm about 31 yr following its outburst, but no source was detected with a  $3\sigma$  limit of  $0.35 \text{ mJy beam}^{-1}$  (Eck, Cowan, & Branch 2002). On the other hand, the VLA detection of SN 1961V at 18 cm about 38 yr after the explosion indicates that it would have been detected with a flux density of  $0.98 \text{ mJy beam}^{-1}$  were it in NGC 2403. Clearly, SN 1961V is more than three times more luminous than SN 1954J at 18-20 cm.

---

<sup>2</sup>The STIS spectrogram has a spectral scale of  $0.554 \text{ \AA pixel}^{-1}$  and a spatial scale of  $0''.05 \text{ pixel}^{-1}$ ; therefore, a  $0''.46$  offset from the slit center corresponds to a wavelength offset of  $0.554 \times 0.46/0.05 = 5.1 \text{ \AA}$ .

Our recent VLBI experiment (§2.2) allows us to make a more definitive radio analysis than previously possible with resolution-limited VLA studies. The VLBI non-detection of SN 1961V indicates that its radio emitting region is larger than the VLBI resolution element; thus the minimum diameter of SN 1961V is 7.56 mas, or 0.34 pc for a distance of 9.3 Mpc. Assuming that the nonthermal radio emission detected by the VLA observations originates from synchrotron radiation associated with SN shocks (Chevalier 1982; Chevalier & Fransson 1994), this minimum size implies an average expansion velocity in excess of 4,400 km s<sup>-1</sup>, between the time of the VLBI experiment and the reported SN explosion, i.e., ~38 yr. This expansion velocity is much higher than the optical expansion velocity of 2,000 km s<sup>-1</sup> measured in 1961 November, toward the end of the broad maximum in the light curve.

Such a large discrepancy in expansion velocities determined at optical and radio wavelengths has been seen previously in SN 1986J, another Type II Peculiar SN. The optical expansion velocity of SN 1986J measured in 1986, several years after its possible explosion in 1982-1983, was less than 1,000 km s<sup>-1</sup> (Rupen et al. 1987). However, VLBI observations of SN 1986J in 1990 and 1999 suggest that its expansion velocity was 20,000 km s<sup>-1</sup> at  $t=0.25$  yr and 6,000 km s<sup>-1</sup> at  $t=15.9$  yr (Bietenholz, Bartel, & Rupen 2002), well in excess of the optical expansion velocity. In the case of SN 1986J, its identification as a SN has been commonly accepted.

### 3.4. The Nature of SN 1961V

Was the SN 1961V event a SN explosion or a super-outburst of an LBV? The strongest support for the SN hypothesis has been provided by radio observations. The nonthermal radio spectral index, high radio luminosity, and the temporal decline of radio luminosity are all consistent with the existence of a decades-old SN. Furthermore, these radio properties are not like those of any known LBV: radio emission from LBVs are predominantly thermal in origin, and LBVs (including SN 1954J) are much fainter than SN 1961V.

The size of SN 1961V’s emitting region may further constrain its nature. Object 7 is unresolved in the *HST* STIS images, placing an upper limit of  $0''.05 = 2.25$  pc on its size. The VLBI non-detection places a lower limit of 7.6 mas = 0.34 pc on the diameter of the radio-emitting region. These sizes are significantly larger than the size of  $\eta$  Car’s nebula in 1995, 0.09 pc  $\times$  0.17 pc, ~150 yr after it was ejected during “The Great Eruption” in 1837-1860 (Humphreys & Davidson 1994; Smith & Gehrz 1998). Whether SN 1961V was a SN explosion or an LBV outburst, the ejected material expands and the expansion velocity can be estimated from the size and time lapse. The above lower and upper limits on size require that the expansion velocity is at least 4,000 km s<sup>-1</sup> but at most 27,000 km s<sup>-1</sup>. Such



high expansion velocity is consistent with a SN explosion, but not an LBV outburst.

The hypothesis that SN 1961V was an LBV outburst can be verified only if the LBV survivor can be convincingly identified. Our STIS observations suggest that Object 7 is the most likely candidate for the LBV survivor because it is the closest to the optical and radio position of SN 1961V and is the only stellar object with the  $H\alpha$  emission line detected. However, Object 7 is not as red as  $\eta$  Car after a super-outburst. Using *HST* WFC1 images taken in 1991 December, Filippenko et al. (1995) reported  $V = 24.22$ ,  $R = 23.37$ , and  $I = 23.79$  (errors  $< 0.2$  mag) for Object 7. Using *HST* WFPC2  $F606W$  images taken in 1994 September and  $F450W$  and  $F814W$  images taken in 2002 July, Van Dyk et al. (2002) reported  $B = 24.04$ ,  $V = 23.85$ , and  $I = 23.83$  for Object 7 with errors  $\sim 0.14$  mag. These can be compared to the LBV Variable 12 that was responsible for SN 1954J:  $B = 22.7$ ,  $V = 21.9$ ,  $R = 21.1$ , and  $I = 20.9$  (errors  $\sim 0.2$  mag) in 1999 February (Smith et al. 2001). It is clear that the color of Object 7,  $B - I = 0.21$  at about 41 yr after the light maximum, is not as red as the color of Variable 12,  $B - I = 1.8$  at about 45 yr after the outburst. Because of the color difference, Object 7 at 41 yr after is about 1 mag brighter in  $B$  but 0.6 mag fainter in  $I$  compared to Variable 12 at 45 yr after the outburst.

We can also compare the  $H\alpha$  line profile of Object 7 to that of  $\eta$  Car. At the distance of SN 1961V, 9.3 Mpc,  $\eta$  Car would not be resolved from its ejecta; therefore, we have extracted an integrated spectrum of  $\eta$  Car and its surrounding ejecta nebula.<sup>3</sup> The ejecta nebula of  $\eta$  Car shows pronounced [N II] lines relative to the  $H\alpha$  line, but the integrated spectrum of the star and the ejecta nebula is dominated by the stellar  $H\alpha$  emission and the nebular [N II] lines become negligible. Figure 3 shows that the  $H\alpha$  line profile of Object 7 is remarkably similar to that of  $\eta$  Car. The lack of a [N II] counterpart to the  $H\alpha$  emission from Object 7 indicates that the emitting material is dense and must be stellar, as is the case for LBVs or mass-losing stars in general. Unfortunately, the previous observations of the  $H\alpha$  line of SN 1961V made by Goodrich et al. (1989) in 1986 were of much lower spectral and spatial resolution, so that the  $H\alpha$  and [N II] lines were blended and heavily contaminated by bright H II region emission. It is impossible to determine whether the  $H\alpha$  line width evolved from 1986 to present.

Is Object 7 an LBV? While its  $H\alpha$  line profile resembles that of  $\eta$  Car, its color is not red. In fact, based on its colors and magnitudes Filippenko et al. (1995) assigned a spectral type of A2 Ib to Object 7. It is interesting to note that there exist A-type supergiants with similar

---

<sup>3</sup>The echelle spectrograph on the 4m telescope at the Cerro Tololo Inter-American Observatory was used to map the kinematics of the ejecta nebula of  $\eta$  Car in the  $H\alpha$  and [N II] lines in 1996 January by Chu et al. The spectral resolution, determined from the FWHM of the sky lines was  $\sim 12$  km s<sup>-1</sup>. Parts of the data were published by Weis, Duschl, & Chu (1999).

H $\alpha$  emission line profiles. For example, the A5 Ia-O star B324 in M33 shows an H $\alpha$  emission line with a narrow core and broad wings, but M33 B324 is not known to exhibit variability and cannot be classified as an LBV (Humphreys, Massey, & Freedman 1990; Herrero et al. 1994). Similarly, the *HST* photometric measurements of Object 7 by Filippenko et al. (1995) and by Van Dyk et al. (2002) do not show significant variations from 1991 to 2002. The lack of large-amplitude variability from 30 yr to 40 yr after the light maximum is in sharp contrast with the variability of  $\eta$  Car after its Great Eruption. Therefore, even if Object 7 is an LBV in a dormant state, its blue color and lack of variability are unlike known LBVs that have gone through super-outbursts, such as  $\eta$  Car.

What is the nature of the SN 1961V event? The radio observations indicate the existence of a decades-old SN. It is possible that the SN exploded in 1961 and was responsible for the light maximum of SN 1961V. It is also possible that the SN exploded prior to 1961 and did not contribute directly to the light curve of SN 1961V. In the latter case, the light maximum of SN 1961V might be caused by a catastrophic but not fatally-explosive event of a massive star, then the spatial coincidence would make Object 7 the most probable candidate for the survivor, but the event cannot have been a super-outburst from an  $\eta$  Car-like LBV. As the radio SN and Object 7 are both coincident with SN 1961V (well within 20 pc), there is a non-negligible possibility that all three objects are related to one another through a binary system similar to the situation in SN 1993J, where a massive binary companion of the SN progenitor is recently identified (Maund et al. 2004). We speculate that Object 7 could be a massive binary companion of the radio SN’s progenitor. Either the SN itself or the SN ejecta impact on Object 7 may be responsible for the light curve of SN 1961V. The impact of SN ejecta on Object 7 injects energy into its atmosphere and causes it to expand and form the broad H $\alpha$  emission line. Similar interactions have been suggested for the binary companions of Type Ia SNe (e.g., Marietta, Burrows, & Fryxell 2000).

We have learned from SN 1961V that the late evolution of massive stars is complex and confusing. Numerous parameters can affect the appearance of a SN or an outburst. Systematic studies of a large number of peculiar SNe are needed. In the meantime, it is necessary to monitor Object 7 photometrically and spectroscopically in the future for variability in order to achieve a better understanding of its nature and relationship with SN 1961V.

#### 4. Summary

We have obtained *Hubble Space Telescope* STIS images and spectra of the stars in the vicinity of SN 1961V. The STIS image shows that SN 1961V and a number of massive stars

are inside a supershell with two H II regions located on the shell rim. Using a new astrometric solution, we find Object 7 of Filippenko et al. (1995) to be the closest to SN 1961V. Furthermore, Object 7 is the only point source detected in our STIS spectra, and only its H $\alpha$  emission is detected. The H $\alpha$  line profile of Object 7 is remarkably similar to that of  $\eta$  Car, but its blue color (similar to an A2 Ib supergiant) and lack of significant variability are unlike any known LBVs at 30-40 yr after a super-outburst.

The nonthermal spectral index and declining radio luminosity of SN 1961V are consistent with those of decades-old SNe. We have obtained VLBA observations of SN 1961V at 18 cm; the non-detection of SN 1961V places a lower limit on the size of the radio-emitting region, 7.6 mas or 0.34 pc. This implies an average expansion velocity in excess of 4,400 km s $^{-1}$ , much higher than the optical expansion velocity measured in 1961. Such discrepant expansion velocities have been observed in other SNe, such as SN 1986J.

We conclude that a SN has occurred in the vicinity of SN 1961V. The physical nature of SN 1961V's light curve remains uncertain. If it was associated with a great eruption of a massive star, Object 7 is the most probable survivor, but its color and lack of significant variability differ from a post-outburst  $\eta$  Car-type LBV. It is possible that the radio SN and Object 7 are both associated with SN 1961V through a binary system. In the future, Object 7 should be monitored photometrically and spectroscopically for variability in order to understand its nature and relationship to SN 1961V.

Support for this work was provided by NASA through grant numbers HST-GO-09371.01-A and HST-GO-09371.02-A from the Space Telescope Science Institute, which is operated by the Association of Universities for Research in Astronomy, Inc., under NASA contract NAS5-26555. Support for this work was also provided in part by NSF, at the University of Oklahoma (AST-0307279).

## REFERENCES

- Bertola, F., & Arp, H. 1970, PASP, 82, 894
- Bietenholz, M. F., Bartel, N., & Rupen, M. P. 2002, ApJ, 581, 1132
- Branch, D., & Cowan, J. J. 1985, ApJ, 297, L33
- Branch, D., & Greenstein, J. L. 1971, ApJ, 167, 89
- Chevalier, R. A. 1982, ApJ, 259, 302

- Chevalier, R. A. & Fransson, C. 1994, *ApJ*, 420, 268
- Cowan, J. J., Henry, R. B. C., & Branch, D. 1988, *ApJ*, 329, 116
- Cowan, J. J., Roberts, D. A., & Branch, D. 1994, *ApJ*, 434, 128
- Duncan, R. A. & White, S. M. 2002, *MNRAS*, 330, 63
- Duncan, R. A. & White, S. M. 2003, *MNRAS*, 338, 425
- Duncan, R. A., White, S. M., & Lim, J. 1997, *MNRAS*, 290, 680
- Duncan, R. A., White, S. M., Lim, J., Nelson, G. J., Drake, S. A., & Kundu, M. R. 1995, *ApJ*, 441, L73
- Eck, C. R., Cowan, J. J., & Branch, D. 2002, *ApJ*, 573, 306
- Fesen, R. A. 1985, *ApJ*, 297, L29
- Fesen, R. A. et al. 1999, *AJ*, 117, 725
- Filippenko, A. V., Barth, A. J., Bower, G. C., Ho, L. C., Stringfellow, G. S., Goodrich, R. W., & Porter, A. C. 1995, *AJ*, 110, 2261
- Freedman, W. L. et al. 2001, *ApJ*, 553, 47
- Goodrich, R. W., Stringfellow, G. S., Penrod, G. D., & Filippenko, A. V. 1989, *ApJ*, 342, 908
- Gruendl, R. A., Chu, Y.-H., Van Dyk, S. D., & Stockdale, C. J. 2002, *AJ*, 123, 2847
- Herrero, A., Lennon, D. J., Vilchez, J. M., Kudritzki, R. P., & Humphreys, R. H. 1994, *A&A*, 287, 885
- Humphreys, R. M., & Davidson, K. 1994, *PASP*, 106, 1025
- Humphreys, R. M., Massey, P., & Freedman, W. L. 1990, *AJ*, 99, 84
- Klemola, A. R. 1986, *PASP*, 98, 464
- Marietta, E., Burrows, A., & Fryxell, B. 2000, *ApJS*, 128, 615
- Maund, J. R., Smartt, S. J., Kudritzki, R. P., Podsiadlowski, P., & Gilmore, G. F. 2004, *Nature*, 427, 129
- Perley, R., Butler, B. J. & Zijlstra, A. 2004, in preparation

- Retallack, D. S. 1983, MNRAS, 204, 669
- Rupen, M. P., van Gorkom, J. H., Knapp, G. R., Gunn, J. E., & Schneider, D. P. 1987, AJ, 94, 61
- Silbermann, N. A., et al. 1996, ApJ, 470, 1
- Smith, N. & Gehrz, R. D. 1998, AJ, 116, 823
- Smith, N., Humphreys, R. M., & Gehrz, R. D. 2001, PASP, 113, 692
- Stockdale, C. J. 2001, PhD thesis, University of Oklahoma
- Stockdale, C. J., Goss, W. M., Cowan, J. J., & Sramek, R. A. 2001a, ApJ, 559, L139
- Stockdale, C. J., Rupen, M. P., Cowan, J. J., Chu, Y.-H., & Jones, S. S. 2001b, AJ, 122, 283
- Tully, R. B. 1980, ApJ, 237, 390
- Van Dyk, S. D., Filippenko, A. V., & Li, W. 2002, PASP, 114, 700
- Weis, K., Duschl, W. J., & Chu, Y.-H. 1999, A&A, 349, 467
- Zwicky, F. 1964, ApJ, 139, 514

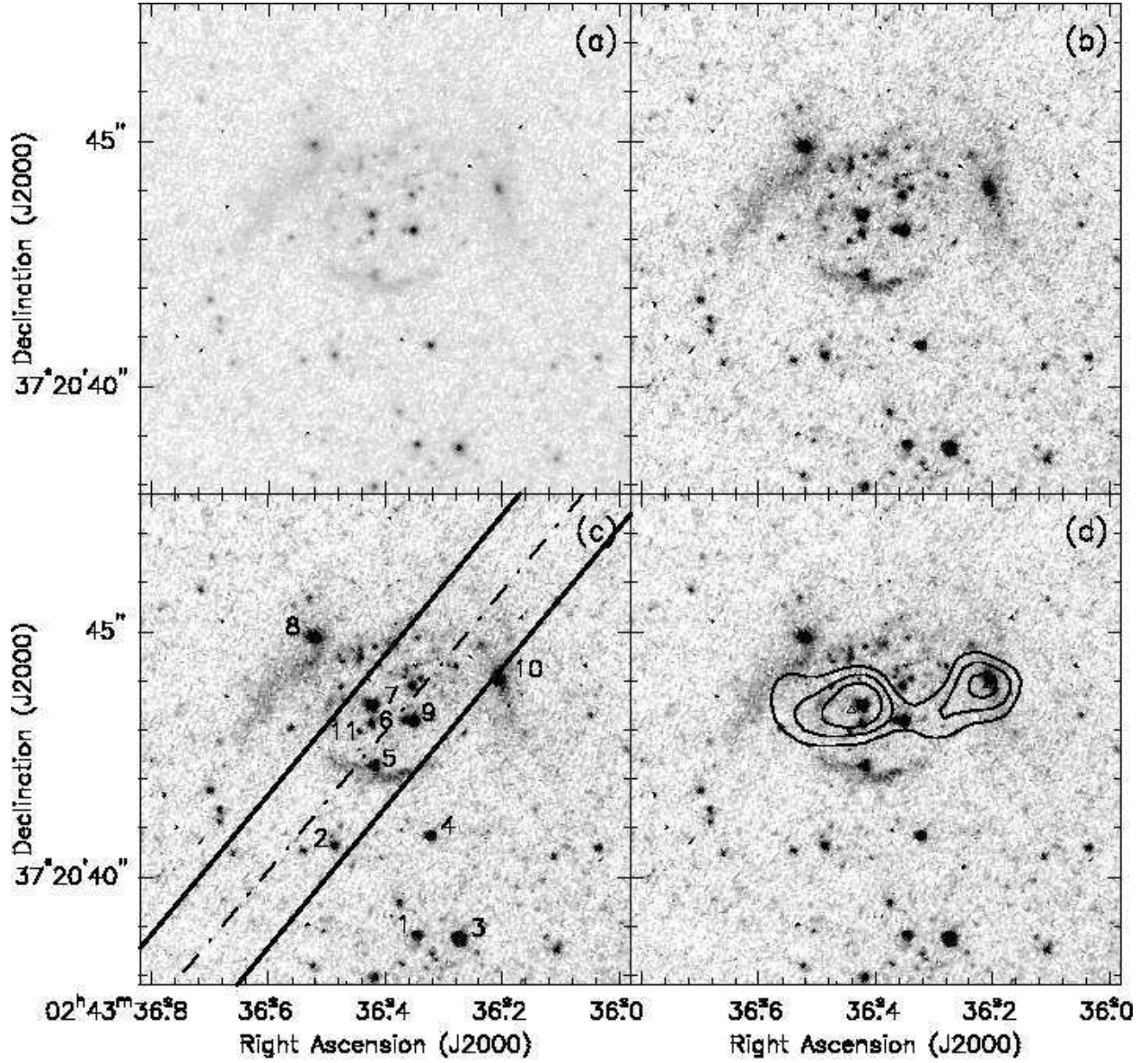


Fig. 1.— *HST* STIS image of the region around SN 1961V. The images are presented in two different greyscales in (a) and (b). The objects identified by Filippenko et al. (1995) and Van Dyk et al. (2002) are marked in (c). The slit position for the STIS spectroscopic observations are also marked in (c). The contours of the VLA 18-cm map observed on 1999 September 14 (Fig. 1b of Stockdale et al. 2001b) are plotted over the STIS image in (d).

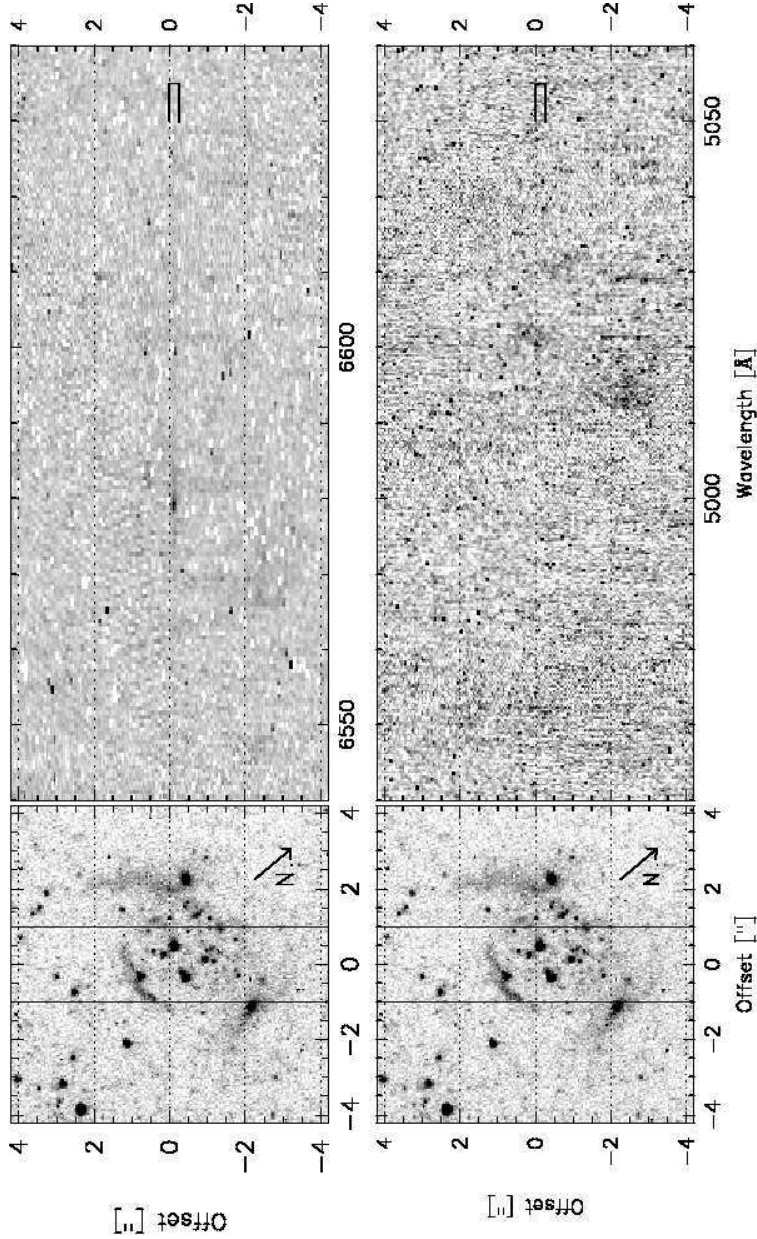


Fig. 2.— *HST* STIS image (left panels) and spectra (right panels) of objects around SN1961V. The direction of north and the 2''-wide slit are marked on the STIS image. The upper right panel shows the spectrum around the H $\alpha$  line and the lower right panel the [O III] lines. Object 7 is the only point source detected, and only its H $\alpha$  emission line is detected. The square bracket marks the slit extent over which the spectrum of Object 7 shown in Figure 3 is extracted. A patch of diffuse emission at slit offset of  $-2''$  to  $-3''$  is detected in both the H $\alpha$  and the [O III] lines. Horizontal dashed lines are drawn to assist in the visual alignment of image and spectral features.

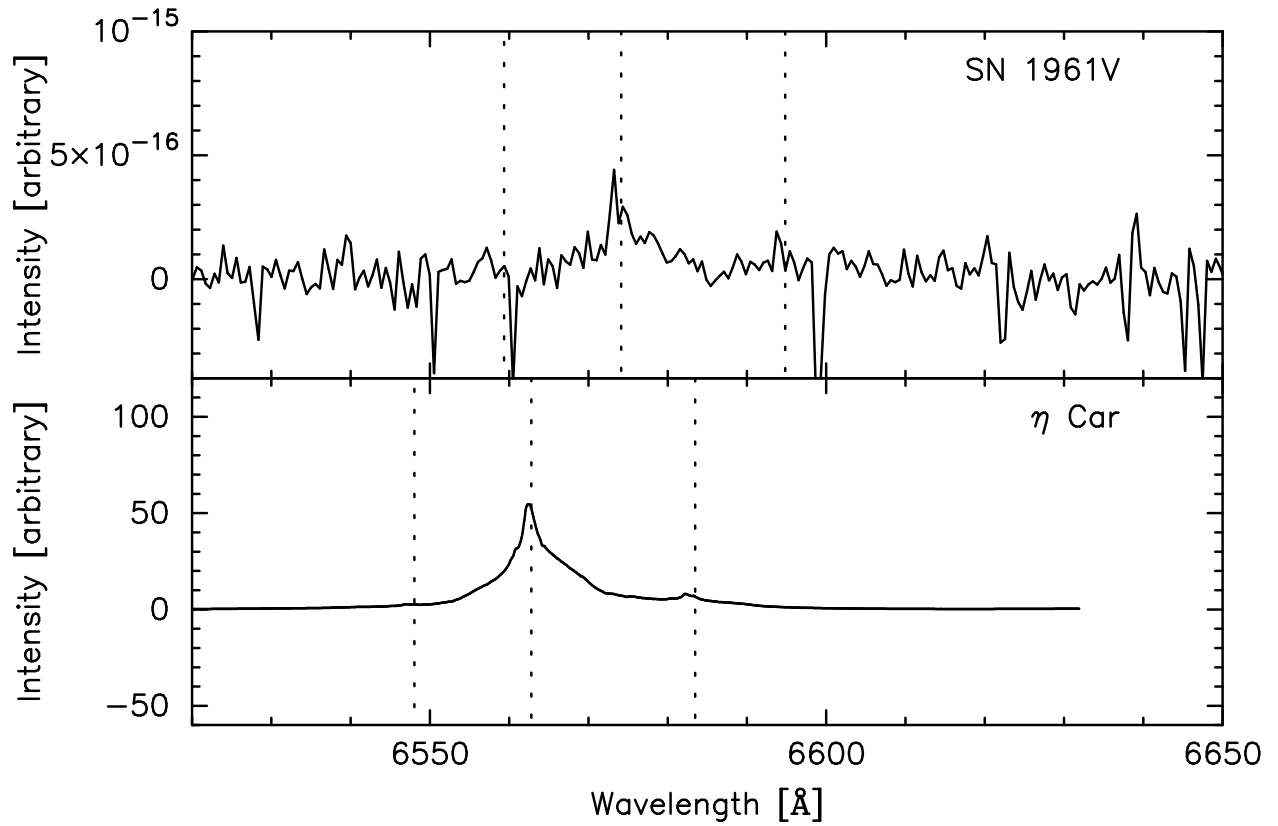


Fig. 3.— (a) H $\alpha$  line profile of Object 7 extracted from our *HST* STIS observations. (b) H $\alpha$  line profile of  $\eta$  Car and its surrounding ejecta nebula taken with the echelle spectrograph on the CTIO 4m telescope. The vertical dashed lines mark the locations of the H $\alpha$  and [N II]  $\lambda\lambda 6548, 6583$  lines.